Research Square

Preprints are preliminary reports that have not undergone peer review.
They should not be considered conclusive, used to inform clinical practice,
or referenced by the media as validated information.

Thermoanalytical and chemical study of the spray-dried extract of Momordica charantia Linn. collected in the Brazilian Amazon

Thiago Leite Silva
Federal University of Para
Alessandra Pantoja Lisboa
Federal University of Para
Ana Carolina Gomes Albuquerque de Freitas
Federal University of Para
Wandson Braamcamp Souza Pinheiro
Federal University of Para
Manolo Cleiton Costa Freitas
Marajó-Breves University Campus, Federal University of Pará
Taís Vanessa Gabbay Alves
Federal University of Para
Attilio Converti
University of Genoa
Roseane Maria Ribeiro-Costa
Federal University of Para
Wagner Luiz Ramos Barbosa
Federal University of Para
José Otávio Carrera Silva-Júnior
carrera@ufpa.br

Federal University of Para

Research Article

Keywords: São-Caetano melon, terpenoids, phenolic compounds, drying, Amazon

Posted Date: July 10th, 2026

DOI: https://doi.org/10.21203/rs.3.rs-9828845/v1

License: This work is licensed under a Creative Commons Attribution 4.0 International License.
Read Full License

Additional Declarations: No competing interests reported.

Thermoanalytical and chemical study of the spray-dried extract of Momordica charantia Linn. collected in the Brazilian Amazon

Thiago Leite da Silva[1], Alessandra Pantoja Lisboa[2], Ana Carolina Gomes de Albuquerque de Freitas[1], Wandson Braamcamp de Souza Pinheiro[3], Manolo Cleiton Costa de Freitas[4], Taís Vanessa Gabbay Alves[1], Attilio Converti[5], Roseane Maria Ribeiro-Costa[6], Wagner Luiz Ramos Barbosa[2], José Otávio Carrera Silva-Júnior*[1]

[1] Laboratory of Pharmaceutical and Cosmetic R&D, Federal University of Pará, Belém 66075-110, Brazil; thiago.leite@ics.ufpa.br; albuquerqueacg@ufpa.br; taisgabbay@ufpa.br; carrera@ufpa.br

[2] Laboratory of Chromatography and Mass Spectrometry, Federal University of Pará, 66075-110, Belém, Brazil; pantoja.lisboa@gmail.com; barbosa@ufpa.br

[3] Central Laboratory of Extraction, Federal University of Pará, 66075-110, Belém, Brazil; wbraamcamp@ufpa.br

[4] Faculty of Natural Sciences, Marajó-Breves University Campus, Federal University of Pará, 68800-000 Breves-PA, Brazil; manolo@ufpa.br

[5] Department of Civil, Chemical and Environmental Engineering, Pole of Chemical Engineering, University of Genoa, Via Opera Pia 15, I-16145 Genova, Italy; converti@unige.it

[6] Laboratory of Pharmaceutical Nanotechnology, Federal University of Pará, 66075-110, Belém, Brazil; rmrc@ufpa.br

*Correspondence: carrera@ufpa.br; +5591 98831-2040

Abstract: *Momordica charantia* (Linn.) is a plant species native to Asia and found in several countries, including Brazil. Its uses, in the form of juice or plant extract, are associated with biological activities such as antidiabetic, analgesic, antiviral, and antiparasitic effects. Spray drying is one of the methods used in the development of formulations, largely due to its ability to microencapsulate active substances, preserving their chemical composition and activity. Thus, this study aims to characterize the thermoanalytical properties of the crude and dried extracts, as well as to identify bioactive compounds using HPLC and NMR. The NMR spectrum confirmed the presence of momordicoside K and rutin in the extracts; the latter compound was also identified in the HPLC chromatogram. Thermal analysis confirmed that spray drying was decisive in improving the thermal stability of the extract compared to the plant

material; furthermore, FT-IR showed the incorporation and compatibility of hydroxyethyl cellulose in the extract. In this regard, these findings suggest that the Amazonian variety of *M. charantia* possesses medicinal potential, given its chemical composition, and that spray drying can be applied as an effective method in the development of herbal pharmaceutical formulations.

Keywords: São-Caetano melon; terpenoids; phenolic compounds; drying; Amazon.

Statements and Declarations: The authors declare no conflict of interest.

Acknowledgments: The authors are grateful to the National Council for Scientific and Technological Development (CNPQ), Coordination for the Improvement of Higher Education Personnel (CAPES), and Dean of Graduate Studies and Research, Federal University of Pará, Belém, Brazil (PROPESP/UFPA).

Funding: The Article Processing Charge for the publication of this research was funded by the Coordenação de Aperfeicoamento de Pessoal de Nivel Superior (CAPES), Brazil (ROR identifier:00x0ma614).

INTRODUCTION

Momordica charantia Linn. is a climbing plant native to eastern India and southern China, belonging to the Cucurbitaceae family [1]. The genus name, *Momordica*, refers to the irregular shape of the leaves, which have a wide range of therapeutic applications [2].

The literature discusses various medicinal uses associated with the species, such as antidiabetic, antioxidant, and antitumor activities, as well as analgesic, abortifacient, antiviral, and HIV-inhibitory effects [3–6]. Although not native to the Brazilian Amazon region, the plant is used topically as an anti-inflammatory and scabicide and is commonly known as “São Caetano melon” [7,8]. In this regard, research on the relationship of the variety cultivated in this region is essential for elucidating the therapeutic effects under study.

Momordica charantia Linn. consists primarily of triterpenoids, particularly cucurbitacins, which are characterized as 19-(10α→9-β)-abeo-10α-lanost-5-ene type systems. In addition, hydroxyl, keto, carboxyl, methoxy, or acetoxy groups can be observed in its main chain, which increases the variability of substances that can be found in the species [9]. However, there has been a notable increase in the number of studies on *Momordica charantia* Linn. highlighting

the presence of considerable levels of phenolic compounds, including flavonoids such as rutin and quercetin, which are associated with various applications [10,11].

Plant extracts are used as pharmaceutical ingredients in various industrial products; however, due to their composition and low stability, the inclusion of drying technologies or their incorporation into controlled-release systems promotes physicochemical stability, improves the distribution and absorption of these substances, regulates the release of the active ingredient, and enhances the therapeutic effect, as well as efficacy and efficiency [12,13].

In this context, the use of drying methods such as spray-drying is evident during the development of new phytotherapeutic formulations. To carry out the process, the plant extract is added together with a drying agent or wall material; these are fed into a drying chamber, where, under specific conditions of temperature, atmosphere, and solution flow, they are atomized, and at this point the extract is encapsulated by the wall material. Thus, the final product—whether the dry extract or the microencapsulated extract—can be characterized as a potential controlled-release system; furthermore, the process improves the material's solubility and, consequently, its pharmaceutical compatibility [14,15].

Therefore, this study aims to obtain and characterize the dry extract of *M. charantia* by spray drying through thermal, spectroscopic, chromatographic, and resonance analyses.

EXPERIMENTAL

Plant Material

The bothanic material was obtained in the City of Belém, latitude 22°46'09.4" S, longitude 49º33'1'' W. Leaves of *M. charantia*, collected from the fresh plant in May 2020, were separated from the other parts, washed in running water, and then dried in the laboratory at room temperature for 24 hours and later in a forced air circulation oven (Solab, SL 102, Piracicaba, Brazil) at 40 °C until constant weight.

Preparation of the Plant Extract

The extraction was performed in accordance with the 2nd edition of Herbal Medicines Form of the Brazilian Pharmacopoeia with some adaptations[16]. Briefly, the material was weighed, moistened with the selected extracting solvent for 1 h and placed in a stainless-steel percolator (MGA, Veranópolis, Brazil). After accommodation of the moistened powder, either absolute ethanol was added in sufficient amount to submerge the powder, which was let to rest

in maceration for 72 h. After this time, percolation was done at a rate of 20 drops per minute. The drip continued until obtaining a tincture with a drug-extract ratio of 1:10 (w/v). The extract was then concentrated in a rotary evaporator (Buchi, R-210, Falwil, Switzerland).

High Performance Liquid Chromatography (HPLC) Analysis

The characterization of the phenolic compounds contained in the sample was performed by HPLC in a HPLC-DAD system, 1260 Infinity (Agilent Technologies, Santa Clara, CA, USA), using a 2 mg/mL solution of rutin in methanol as a standard.

The crude extract of *M. charantia* leaves was previously suspended in dichloromethane and then filtered through a cellulose membrane with 0.22 μm pore diameter (Millipore, Bedford, MA, USA). The injection volume was 20 μL and the separation column was an Xbridge C18 column (4.6 mm × 250 mm, 5 μm) maintained at 39 °C. The mobile phase consisted of a 0.1% aqueous solution of formic acid (Solvent A) and acetonitrile (18-50%) (Solvent B) at a flow rate of 1 mL/min. The peak was detected at a wavelength of 330 nm. Coelution, performed to confirm the identity of the compounds, was carried out with 200 μL aliquots of the rutin solution added after evaporation of the solvent to 1.0 mL of concentrated extract solution.

Nuclear Magnetic Resonance (NMR) Analysis

For NMR analysis, crude extract was treated by solid phase extraction in Strata C18 cartridges (1000 mg/mL) conditioned with 6 mL of acetonitrile (ACN) and then with 6 mL of water. After addition of 4.8 mL of ACN to 150-mg aliquots of each sample, sonication (UP100H, Hielscher, Teltow, Germain) was applied at 100 Watt for 5 min. Then, 1.2 mL of water were added, and sonication was applied again for the same time. Each solution was transferred to a cartridge, to which 14 mL of an ACN:H2O (8:2) solution were subsequently added. The collected solution (20 mL) was evaporated in an exhaust hood.

50 mg of extract were dissolved in 600 μL of deuterated dimethyl sulfoxide (DMSO-d_6) under the same conditions described for HPTLC analysis. NMR spectra (^{1}H and ^{13}C NMR), as well as Homonuclear Correlation Spectroscopy (HOMO-COSY), Heteronuclear Single Quantum Coherence (HSQC) and Heteronuclear Multiple Bond Coherence (HMBC) correlation maps, were obtained using an Ascend™ spectrometer (Bruker, Rheinstetten, Germany), operating at 400 and 100 MHz.

For data control and treatment, the TopSpin 3.6.0 software was used, and the FIDs were subjected to Fourier transform, with line broadening (LB) of 0.3 Hz. The spectra were manually treated, baseline corrected and calibrated, having as internal reference the residual signal of DMSO at 2.49 ppm (^{1}H) and 39.5 ppm (^{13}C). In the FIDs processing, the abundance of functional groups present in the phytochemical classes of interest was also investigated, grouping them into specific regions (δ = 0.5 – 1.5 / 1.5 – 3.0 / 3.0 – 4.5 / 4.5 – 6.0 / 6.0 – 9.0 / 9.0 – 10.0 ppm), and the integrals of the respective regions were normalized [17].

For signal identification, chemical shift data (δ) and coupling constants (*J*) of one-dimensional (1D) spectra of ^{1}H and ^{13}C were used, in addition to two-dimensional (2D) correlation maps ^{1}H (HOMO-COSY), ^{1}H ^{13}C (HSQC) and ^{1}H ^{13}C (HMBC).

Obtaining the Dry Extract by Atomization

For spray drying, the M. charantia tincture was homogenized with hydroxyethyl cellulose (HEC) (PharmaNostra®) at concentrations of 0.5%, 0.75%, and 1.5% (w/v). After solubilizing the HEC, distilled water was added to the mixture under stirring to adjust the alcohol content appropriately, in accordance with the manufacturer's instructions. For drying, a Labmaq MSD 1.0® spray dryer (Ribeirão Preto, Brazil) with a co-current flow regime was used under the following conditions: drying air inlet temperature 140°C, atomization air flow rate 33 L.min^{-1}, drying air flow rate 1.68 m^{3}.min^{-1}, mixture feed rate 0.5 mL.min^{-1} as reported by Silva-Júnior et al. [18].

Determination of the Thermoanalytical Profile of Plant Extracts

To evaluate the thermogravimetric profile of the plant material and the dry extract, thermogravimetric analysis (TGA) was performed using a Shimadzu® DTG 60 (Kyoto, Japan). Approximately 3 ± 0.1 mg of each sample was weighed into a platinum crucible and subjected to a temperature range of 25–600 °C under a dynamic nitrogen atmosphere (25.0 mL.min^{-1}) and a heating rate of 10 °C·min^{-1}. The results were expressed as mass loss (%) as a function of temperature (°C) using Shimadzu® TA-60W software (Kyoto, Japan) [19].

Differential scanning calorimetry (DSC) was performed to determine the thermal profile, using a DSC60 Plus model (Shimadzu, Kyoto, Japan). For the analysis, approximately 5.0 ± 0.1 mg of the plant material and the dry extract were weighed into an aluminum crucible and subjected to a temperature range of 25–600 °C with a heating rate of 10 °C.min^{-1} and dynamic nitrogen atmosphere with a flow rate of 50.0 mL.min^{-1}. The results were expressed as heat

151 flow/W.g^{-1} as a function of temperature (°C) using Shimadzu® TA-60W software (Kyoto, Japan)
152 [19].

153 **Fourier-Transform Infrared (FTIR) Profile of Extracts**

154 The FTIR spectra were obtained from samples of the concentrated extracts percolated
155 with both a 70% ethanol-water solution and dry extract [18,19]. Readings were done in the
156 wavenumber range from 4000 to 400 cm^{-1}, using appropriate amounts of the sample. The
157 analyses were performed using a spectrometer IR Prestige-21 (Shimadzu, Kyoto, Japan).

158 **RESULTS AND DISCUSSION**

159 **HPLC and NMR Analyses**

160 The presence of rutin in the sample was confirmed by comparing the HPLC-UV/Vis
161 spectra of the standard (rutin) and the *M. charantia* extract at a retention time (Rt) of 7.457 min.
162 Both samples showed coelution at Rt = 7.241 min (Figure 1) and UV/Vis absorption spectra
163 with high matching to each other (Figure 2). The results are listed in Table 1.

164 The calibration curve constructed for rutin quantification is illustrated in Figure 3. Based
165 on the data obtained from the curves, the detection (DL) and quantification (QL) limits listed
166 in Table 2 were determined.

167 **Table 1.** Parameters found in the HPLC analysis of the ethanolic extract of *Momordica*
168 *charantia* leaves. Rt = retention time.

Compound	Coelution Rt (min)	Sample peak area	Coelution area	Peak resolution	Matching percentage (%)
Rutin	7.241	150.9	532.6	2.65	99.814

169

170

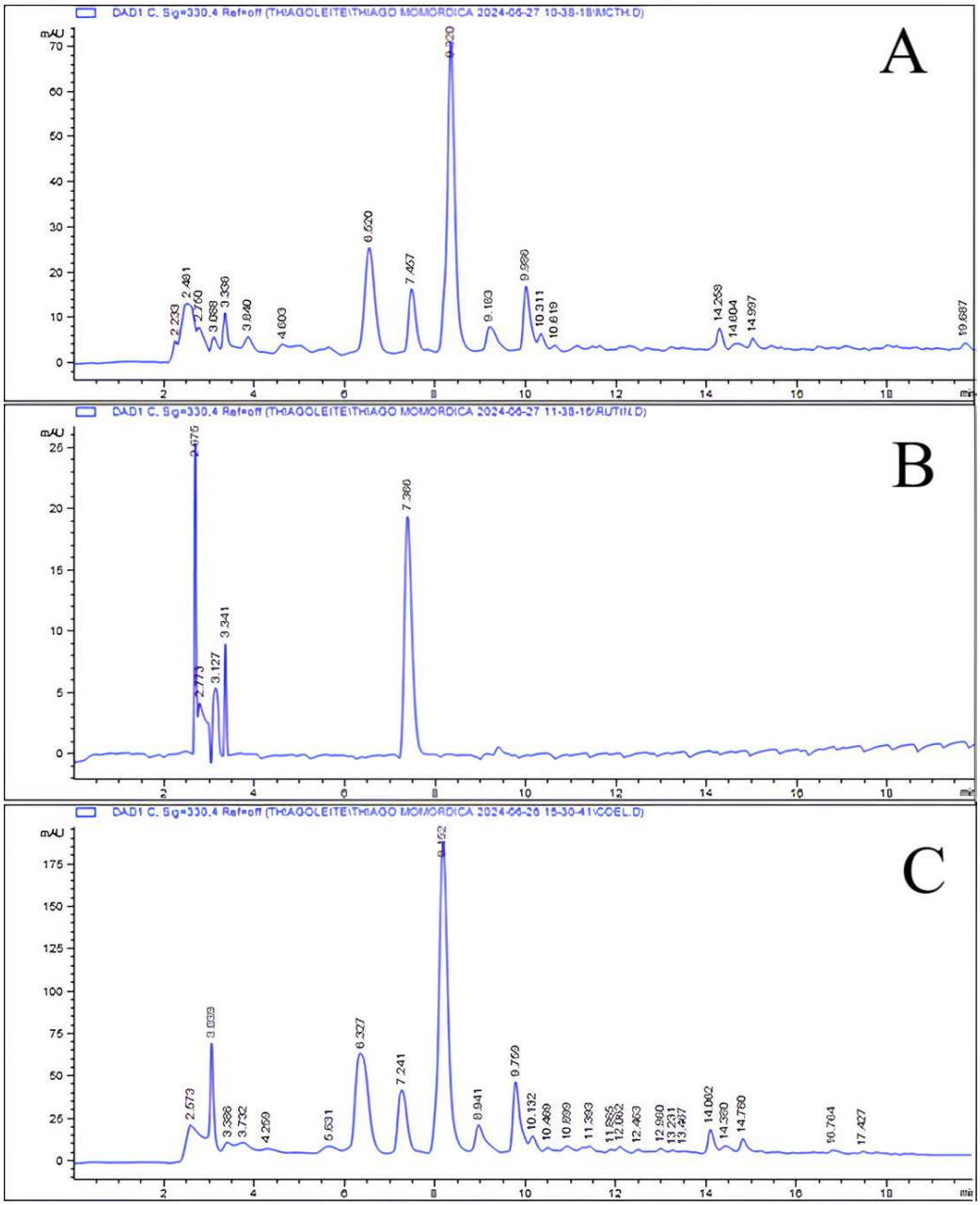


Figure 1. HPLC chromatograms of the concentrated extract of *Momordica charantia* leaves (A), rutin (B) and the extract coeluted with the standard (C), respectively.

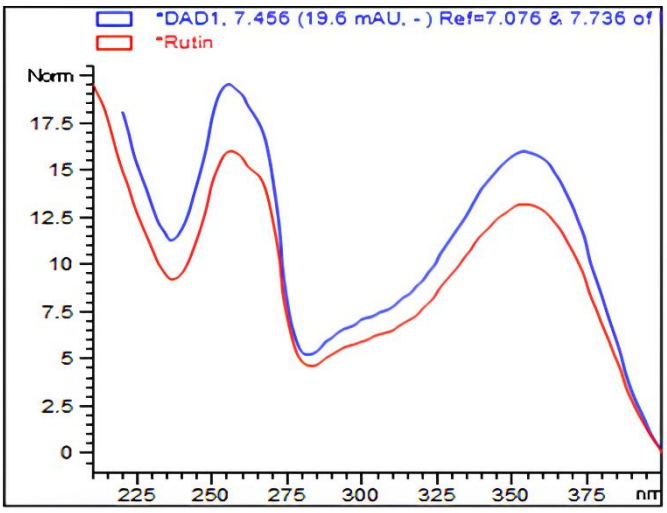


Figure 2. Comparison of UV-Vis spectra of rutin (red) and extract of *Momordica charantia* leaves at a retention time of 7.456 min (blue).

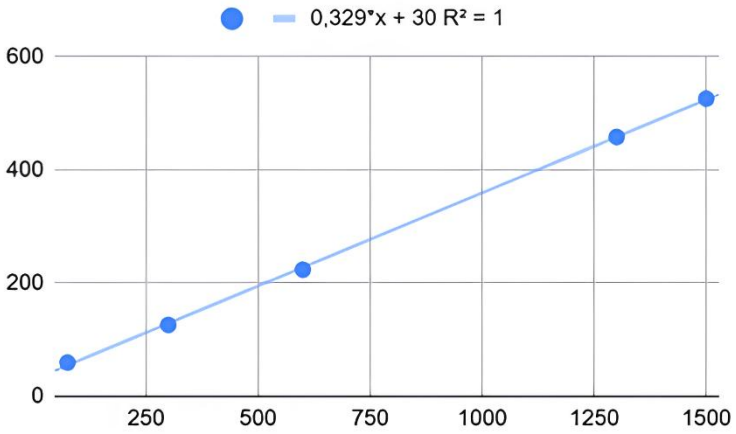


Figure 3. Rutin calibration curve.

Table 2. Values of the determination coefficient (R^2) and of the limits of detection (DL) and quantification (QL) of rutin in the sample.

Compound	R^2	DL (µg/mL)	QL (µg/mL)
Rutin	0.999	1.162	3.522

The spectroscopic profile obtained by ^{1}H and ^{13}C NMR (Figures 4 and 5) allowed to evaluate the chemical composition of the ethanolic extract of *M. charantia* leaves by identifying fragments, or functional groups, as well as their abundances through the integration of signals observed in each region of the spectrum.

Particularly, the 0.5 to 1.5 ppm region of the ^{1}H NMR spectrum, which comprises signals from methyl (-CH_3), methylene (-CH_2) and methine (-CH) hydrogens typical of alkyl groups, accounted for approximately 43.32% of the area under the curve. The 1.5 to 3.0 ppm region, typical of -CH_3, -CH_2 and -CH hydrogens linked to the C=C double bond, to ketone (-COR), aldehyde (-COH) or ester (-COOR) carbonyls, to nitrogen atoms (N) or to aromatic rings (-Ph), accounted for a percent area of 29.85%. The region from 3.0 to 4.5 ppm, typical of hydrogens linked to hydroxylated carbons (-C-OH), or to carbons substituted by alkoxy (RO-C-) or phenoxy (PhO-C-) and acylate (RCOO-C-) groups, was responsible for an area of 9.74%, while that of hydrogens of olefinic groups (CH_2=CH-R and R-CH=CH-R), between 4.5 and 6.0 ppm, represented 7.91% of the total. Another prominent region was that of hydrogens linked to aromatic carbons (Ph-H) or to olefinic carbons vicinal to an aromatic ring (Ph-CH=CH-R), which accounted for 5.75% of the total area of the extract spectrum (Table 3).

The ^{13}C NMR spectrum of the ethanolic extract (Figure 5), performed to corroborate the information from the ^{1}H NMR one, showed signals of aliphatic carbons (-CH_3, -CH_2-, -CH-, CH_3-CO-, -CH_2-NH_2) in the spectral region between 10.0 and 50.0 ppm. On the other hand, in the region from 50.0 to 90.0 ppm, typical of oxidized aliphatic carbons in ethers (-C-O-C-) and alcohols (-C-OH), signals were observed that suggested the presence of sugars, as observed in the ^{1}H NMR (δ_H 3.0 – 4.5 ppm). Finally, in the regions of aromatic and olefinic carbons, from 100.0 to 140.0 ppm, and between 140.0 and 160.0 ppm, typical of oxidized aromatic carbons, the presence of phenolic compounds was inferred.

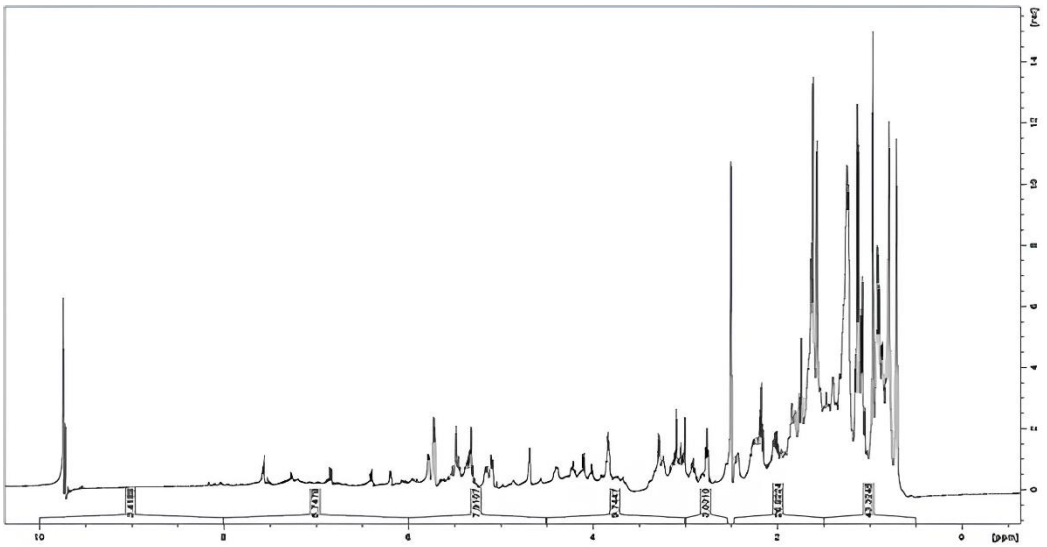


Figure 4. ^{1}H NMR spectrum of the extract of *Momordica charantia* leaves.

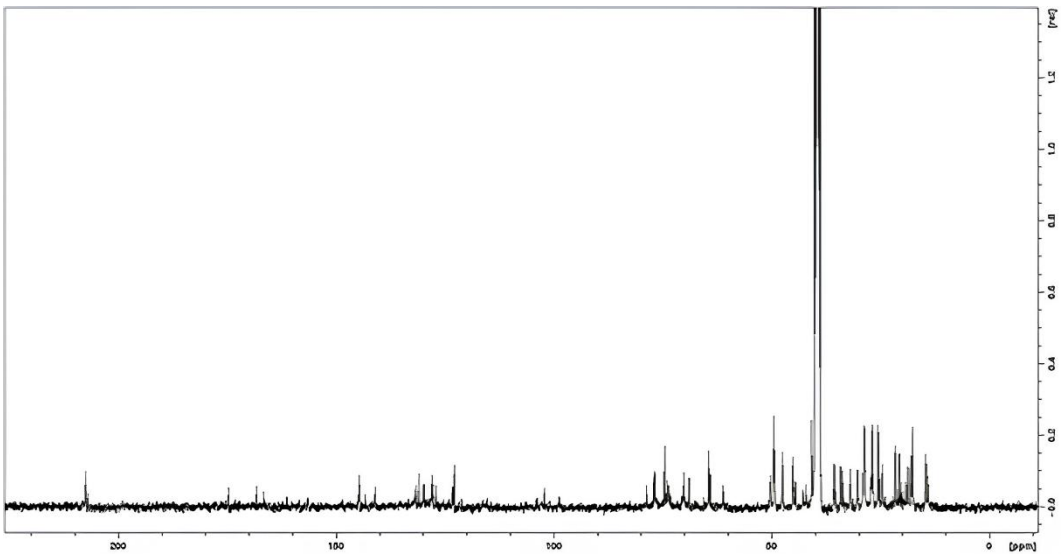


Figure 5. ^{13}C NMR spectrum of the extract of *Momordica charantia* leaves.

The two-dimensional NMR spectra (COSY, HSQC and HMBC) of the ethanolic extract of *M. charantia* leaves allowed demonstrating a certain phytochemical diversity from the analysis of the correlations of the ^{1}H/^{1}H ($^{2,3}J_{H,H}$), ^{1}H/^{13}C ($^{1}J_{C,H}$) and ^{1}H/^{13}C ($^{2,3}J_{C,H}$) signals, which are typical of bonds and fragments present in flavonoids and terpenoids, as well as detecting the presence of two compounds in particular: the flavonol rutin and the triterpene momordicoside K (Figures 6, 7 and 8 and Table 4).

Table 3. Distribution of areas of the ^{1}H NMR spectrum of *Momordica charantia* leaves extract related to structural fragments of substances detected in the analyzed sample.

Chemical shift (ppm)*	Fragment	Area (%)
0.5 – 1.5	C-C**H**$_n$	43.32
1.5 – 3.0	C**H**$_n$-C=C; C**H**$_n$-COR; C**H**$_n$-COOR; C**H**$_n$-N; C**H**$_n$-Ph	29.85
3.0 – 4.5	C**H**$_n$-OH; PhO-C**H**$_n$; RCOO-C**H**$_n$; C**H**$_2$-NHCOR	9.74
4.5 – 6.0	C**H**$_n$=CH	7.91
6.0 – 8.0	Ph-**H**; Ph-C**H**=CH-R	5.75
9.0 – 10.0	R-CO-**H**	3.42

n = number of hydrogens, where $1 \geq n \leq 3$*[17]

The HSQC spectrum highlighted the correlations between the signals of an aromatic ring fragment at δ_H/δ_C (ppm) 6.18 (*d* 2.0) / 98.8, 6.39 (*d* 2.0) / 93.8, 7.57 (*d* 2.1) / 116.7, 6.84 (*d* 8.0) / 116.3 and 7.58 (*dd* 2.1; 8.0) / 122.9, two correlated pairs indicating anomeric H/C at 4.40 (*d* 1.6) / 101.0, and also the typical signals of a rhamnose methyl group at 0.93 (*sl*) / 19.2. These findings suggested the signals came from a glycosylated flavonoid. After confirming the correlations of the COSY ^{1}H/^{1}H ($^{2,3}J_{H,H}$) and HMBC ^{1}H/^{13}C ($^{2,3}J_{C,H}$) spectra, in addition to comparison with literature data [20], it was possible to infer the presence of the glycosylated flavonol rutin (Table 5).

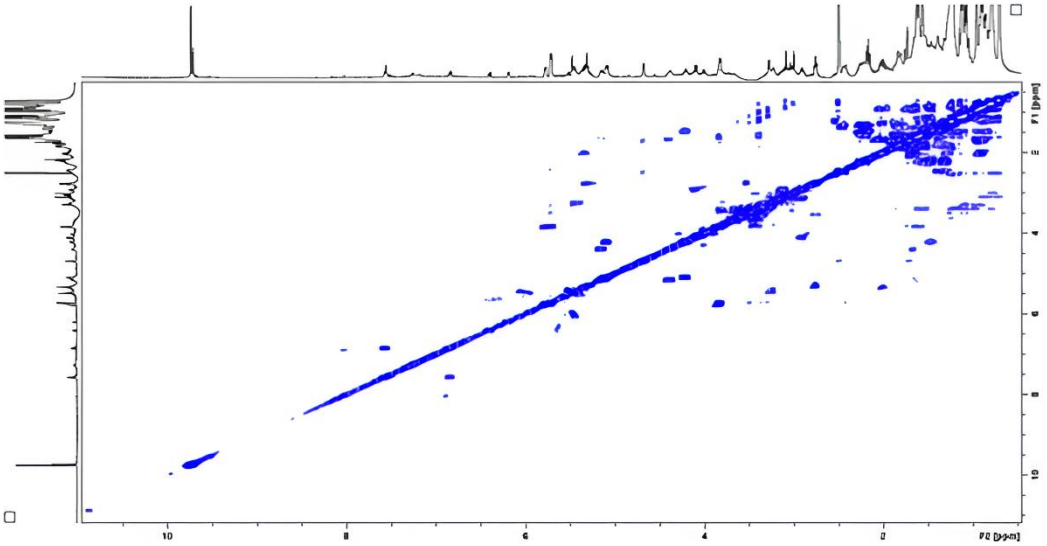


Figure 6. Two-dimensional COSY NMR spectrum of the extract of *Momordica charantia* leaves.

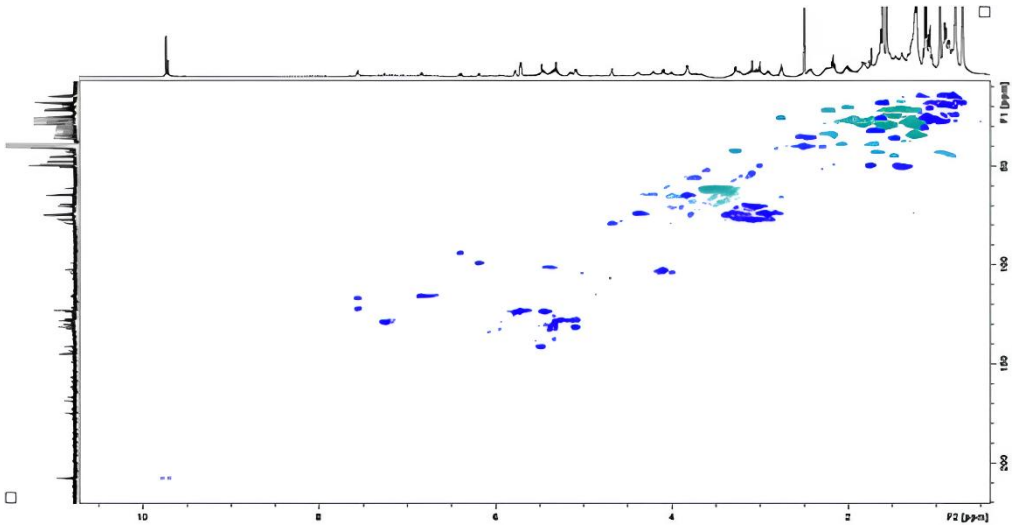


Figure 7. Two-dimensional HSQC-Ed NMR spectrum of the extract of *Momordica charantia* leaves.

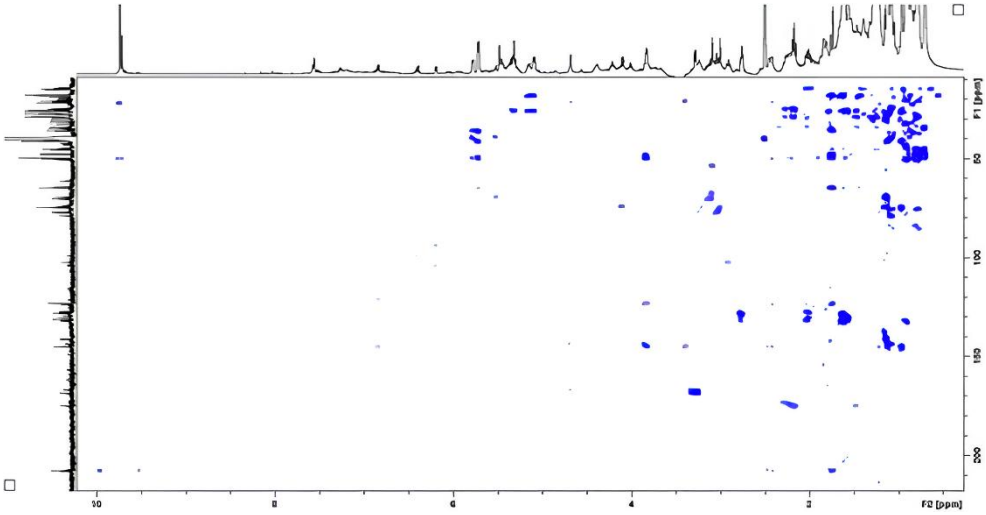
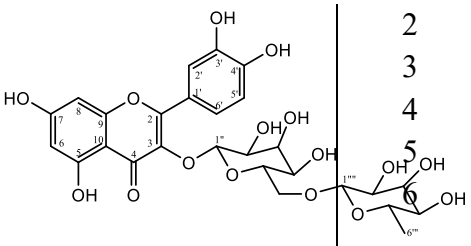
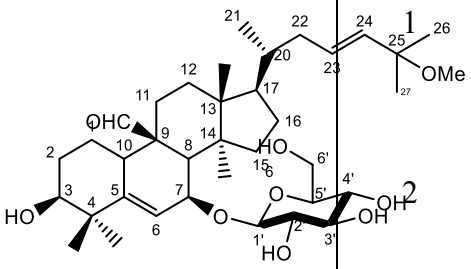


Figure 8. Two-dimensional HMBC NMR spectrum of the extract of *Momordica charantia* leaves.

Table 4. Concentrations of total phenolic compounds and flavonoids in the extract of *M. charantia* leaves

ID	Compound	Position	δ ^{1}H (*J*/Hz)	δ ^{13}C
1	Rutin			

		2	-	156.5
		3	-	133.4
		4	-	177.9
		5	-	161.3
		6	6.18 (*d* 2.0)	98.8
		7	-	164.3
		8	6.39 (*d* 2.0)	93.8
		9	-	156.6
		10	-	103.7
		1’	-	121.3
		2’	7.57 (*d* 2.1)	116.7
		3’	-	145.2
		4’	-	148.6
		5’	6.84 (*d* 8.0)	116.3
		6’	7.58 (*dd* 2.1, 8.0)	122.9
		1”	5.34 (*d* 6.8)	102.3
		1’”	4.40 (*d* 1.6)	101.0
		6’”	0.93 (*sl*)	19.2
2	Momordicoside K			
		1	1.40 (*d* 9.2) Ha 1.32 (*m*) Hb	20.9
		2	1.85 (*m*) Ha 1.50 (*m*) Hb	28.6
		3	3.39 (*m*)	74.4
		4	-	41.0
		5	-	146,6
		6	5.71 (*d* 4.3)	120.8
		7	4.09 (*d* 5,1)	70.3
		8	1.94 (*s*)	43.6
		9	-	49.4

		10	2.45 (*d* 12.6)	35.5
		11	1.32 (*m*) Ha 2.18 (*m*) Hb	21.8
		12	1.54 (*m*) Ha 1.61 (*m*) Hb	28.6
		13	-	44.9
		14	-	47.3
		15	1.32 (*m*) Ha 1.22 (*m*) Hb	33.9
		16	1.30 (*m*) Ha 1.85 (*m*) Hb	26.9
		17	1.45 (*dd* 17.9, 8.9)	49.2
		18	0.81 (*s*)	14.7
		19	9.74 (*s*)	207.4
		20	1.55 (*m*)	35.5
		21	0.88 (*d* 6.2)	18.6
		22	1.77 (*m*) Ha 2.13 (*d* 13.3) Hb	38.8
		23	5.48 (*m*)	127.6
		24	5.35 (*d* 13.5)	136.9
		25	-	74.2
		26	1.16 (*s*)	26.1
		27	1.16 (*s*)	25.6
		OMe	3.00 (*s*)	49.2
		1’	4.10 (*d* 7.8)	102.2

253

In the ^{13}C NMR and HSQC-Ed spectra, six spectral lines typical of quaternary carbons were also observed, in addition to eight characteristic signals of methylene carbons (CH_2) at δ_C (ppm) 14.7, 17.7, 18.6, 20.9, 21.8, 25.5, 25.6, 26.1, 26.8, 26.9, 28.6 and 28.6, as well as seven other typical signals of methyl carbons. Thus, it was concluded that a triterpene structure was present. Furthermore, the observed correlation of the anomeric hydrogen δ_H-6a signal at 99.9 ppm is a characteristic bridge of acetal carbon (O–CH–O) and oxidized aliphatic carbons at δ_C between 61.2 and 78.8 ppm typical of a glycosylated triterpene.

Furthermore, the ^{13}C NMR spectrum revealed four signals at δ_C (ppm) 120.8, 127.6, 136.9 and 146.6, indicating a molecule with two double bonds. Combining with the HSQC mapping, correlations with signals at δ_H (ppm) 5.71 (*d*, 4.3), 5.48 and 5.35 were evident. The correlation of the C-6 signal at δ_C 120.8 ppm and HMBC showed interaction of H6 with C4, C7 and C10, proving that one of the double bonds was located between C5 and C6, while, based on HMBC mapping, the interaction of C24 with H26 and H27 allowed positioning the other between C23 and C24. Furthermore, H24 at 5.35 ppm (*d* 13.5) demonstrated that H23 and H24 were in *trans* position.

The ^{13}C NMR spectrum showed the C19 signal at 206.4 ppm, which is characteristic of the aldehyde group, while HMBC showed the interaction between H8 and C19, suggesting that the aldehyde group was bound at position 9. After confirming the correlations of the COSY $^{1}H/^{1}H$ ($^{2,3}J_{H,H}$) and HMBC $^{1}H/^{13}C$ ($^{2,3}J_{C,H}$) spectra, comparison with literature data [20] allowed deducing the structure of momordicoside K (Table 5).

The presence of rutin in the *M. charantia* leaf extract was confirmed by NMR and HPLC analysis, the later which also allowed the detection of other phenolic compounds analogous to rutin and *p*-coumaric acid.

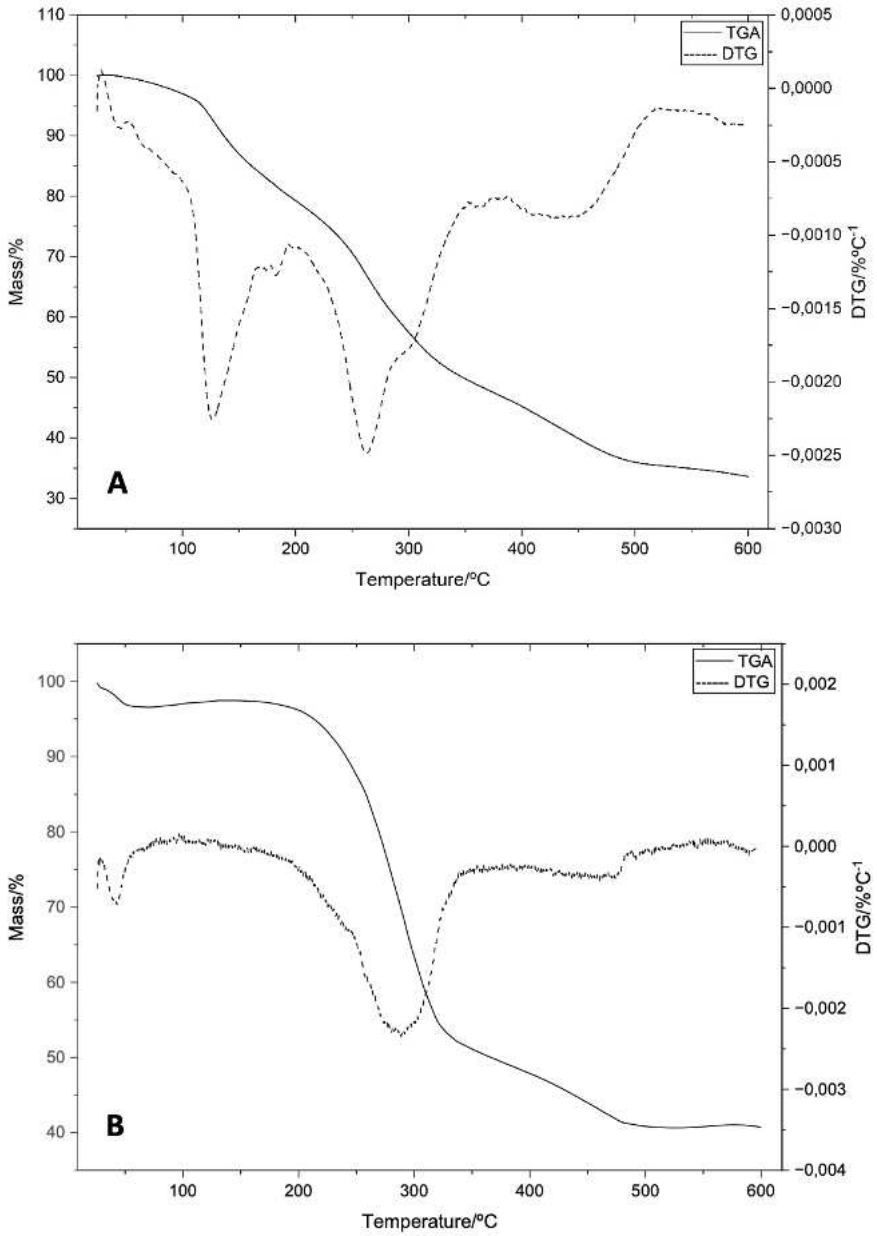
NMR spectra also confirmed the presence of momordicoside K, one of the cucurbitacins characteristic of the species under investigation [21,22]. Several studies have demonstrated the presence of terpenoids in different extracts, several of which characterized by NMR. Nhiem et al.[23] isolated three triterpenoids from *M. charantia*, using NMR analysis for their identification. Following the same line, Liao et al.[24] also identified two triterpenoids using the same technique. Several other studies have reported the presence of triterpenoids in this species, not only describing their structures, but also relating them to important biological activities [25,26].

285 **Thermal Analysis Profile of the Extracts**

286 Figure 9A shows the thermal behavior of the *M. charantia* plant material as determined
287 by thermogravimetric analysis. In this figure, three mass loss events can be observed (Table 6);
288 the first event, with a loss of approximately 7.24%, is related to the evaporation of water and
289 volatile substances. It should be noted that this percentage is in line with expectations for plant
290 materials, for which the limit is 10% [27,28]. Furthermore, it should be noted that excess water
291 may contribute to potential microbiological contamination.
292 The second event observed occurred between the on-set temperature (251.56°C) and end-
293 set temperature (363.03°C), accounting for 51.60% of the mass loss, and the third event
294 occurred between 408.55°C and 447.81°C, with a mass loss of 23.25%. These events are related
295 to the degradation and decomposition of the carbon chains of the metabolites characteristic of
296 the species [19].

297 Figure 9B, on the other hand, shows the thermogravimetric profile of the dry extract of
298 M. charantia, in which two mass loss events are observed. The first event (Table 5) occurs at
299 on-set (31.87°C) and end-set (59.80°C) temperatures, accounting for 4.70% mass loss, and the
300 second event occurs between 235.08°C and 281.36°C with 52.03% mass loss. These are related
301 to the evaporation of residual water and the degradation of carbon chains, respectively [19]. It
302 should be noted that the dry extract was much more thermally stable; this characteristic may be
303 related to the process of encapsulating the sample in hydroxyethylcellulose, suggesting that it
304 is an excellent wall material. Similar results were found in the study by Silva-Júnior et al. [18],
305 who microencapsulated the extract of Symphytum officinale L. using hydroxyethylcellulose as
306 a drying adjuvant and observed mass losses in events similar to those in this study.

307



308

309 **Figure 9:** Thermogravimetric analysis A) crude extract; and B) M. charantia extract.

310 **Table 5:** Thermal analysis profile of the crude extract and the dry extract of

311 *Momordica charantia*

TGA Analysis				
Sample	Event	Temperature Onset (°C)	Temperature Endset (°C)	Mass loss (%)
Crude extract	1	113.64	128.45	7.24

	2	251.56	363.03	51.60
	3	408.55	447.81	23.25
Dry extract	1	31.87	59.80	4.70
	2	235.08	281.36	52.03

DSC Analysis

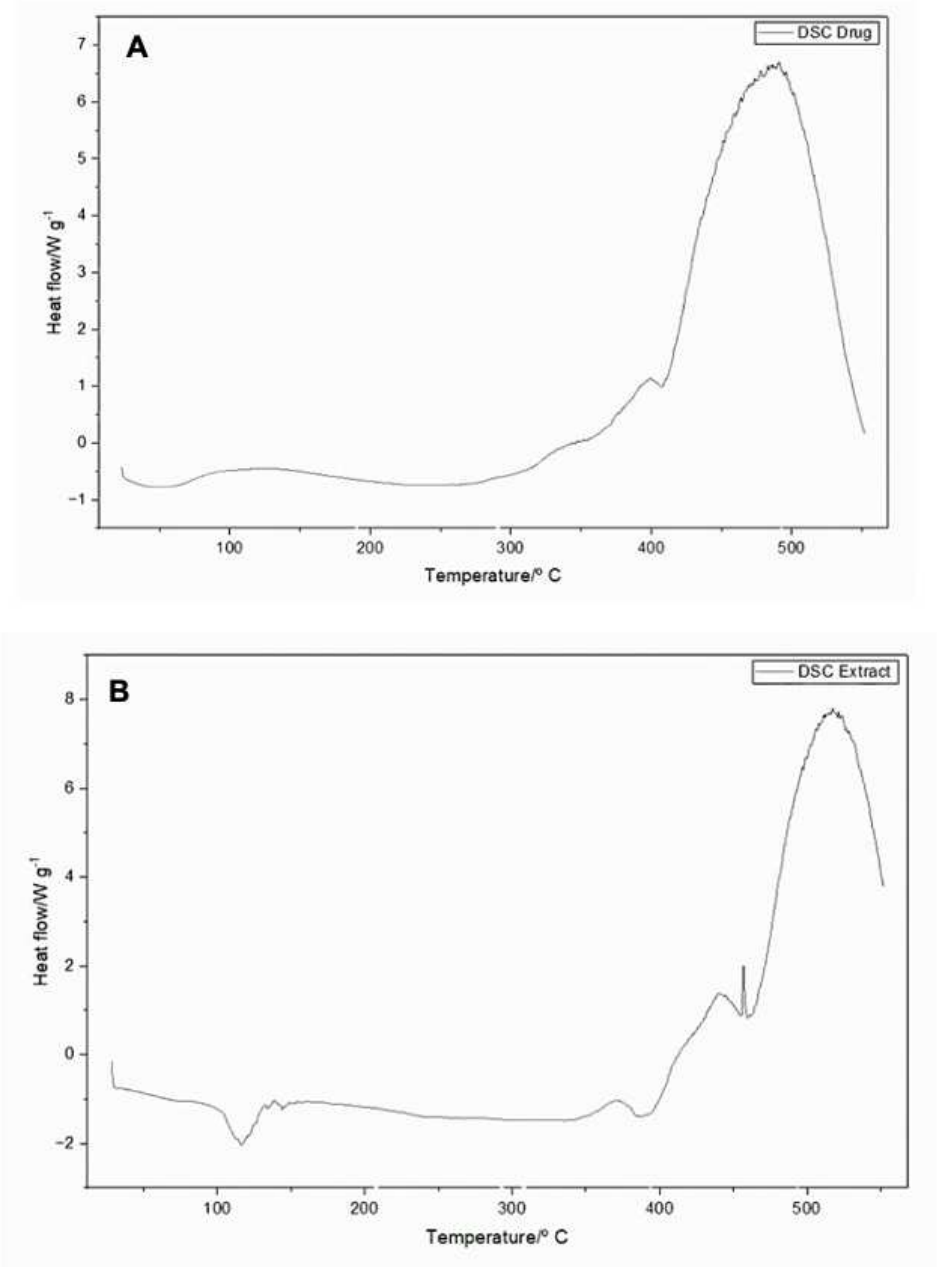
Sample	Event	Temperature Onset (°C)	Temperature Endset (°C)	Height (mW)
Crude extract	1	383.54	401.67	0.28
	2	417.92	531.13	5.86
Dry extract	1	123.63	133.95	-0.88
	2	359.53	384.20	0.36
	3	455.97	458.15	1.10
	4	474.95	547.57	4.92

Figure 10A shows the two endothermic events of the crude extract, occurring in the temperature range of 383.54 – 401.67 °C and 417.92–531.13 °C, respectively. These events are consistent with the TGA, a range in which the degradation and decomposition of secondary metabolites and carbon compounds present in the plant material are observed. It should be noted that the first event exhibits Heat 27.70 $J \cdot g^{-1}$and Heat 0.28 mW, while the second event exhibits Heat 2.25 $KJ \cdot g^{-1}$and Heat 6.86 mW (Table 6) [19].

Figure 10B, on the other hand, shows four events in the dry extract. The first event occurs between 123.63–133.95 °C and is an exothermic event with Heat -49.35 $J \cdot g^{-1}$ and Heat -0.88 mW; this event is consistent with the TGA, where a subtle drop in the curve can be observed within the same temperature range. The remaining events are endothermic with Heat 21.74; 4.68; and 881.53 $J \cdot g^{-1}$ and Heat 0.36; 1.10; and 4.92 mW, for events 2, 3, and 4, respectively (Table 5). These events are related to polymer degradation, as well as the degradation and decomposition of secondary metabolites and carbon compounds present in the

326 plant material [19].

327



328

329 **Figure 10:** DSC analysis of A) plant material; and B) M. charantia extract.

330 **FTIR Analysis**

331 The FTIR spectra of the ethanolic extract of *M. charantia* prepared using absolute ethanol is
332 shown in Figure 11A, where one can observe a main band around 2920 cm^{-1} and several other
333 bands between 1200 and 912 cm^{-1}. The latter region, known as the fingerprint zone, showed
334 peaks between 1020 and 1075 cm^{-1}, in addition to those around 1150, 1100 and 1050 cm^{-1}, and
335 at 1200 cm^{-1}. Finally, a set of vibrations around 600 cm^{-1} was also observed.

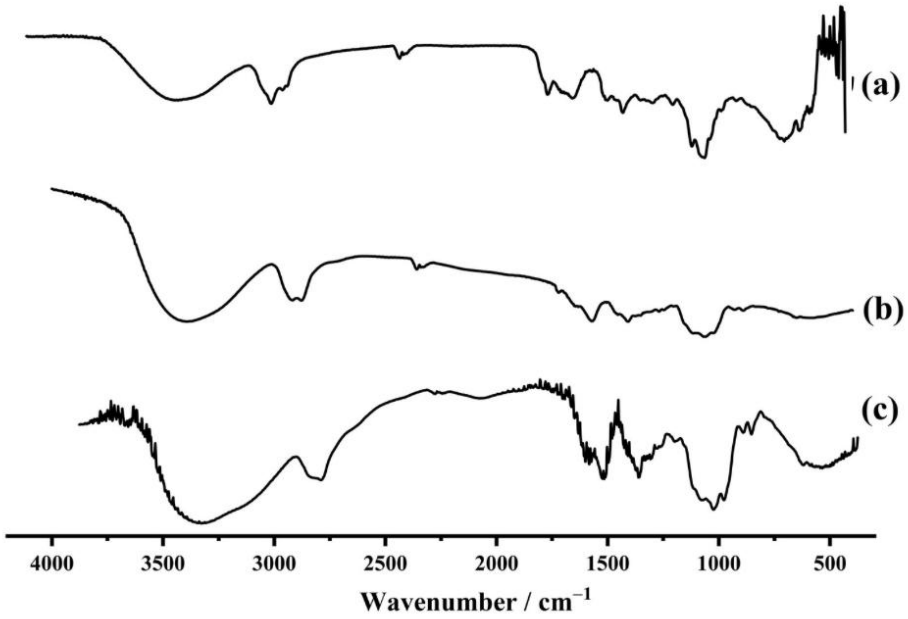


Figure 11. FTIR spectra of: a) the ethanolic extract; b) dry extract of *Momordica charantia* leaves; and c) hydroxyethylcellulose.

Examining the FTIR spectra in Figure 11A and 11B, bands can be observed in regions that indicate the presence of phenolic compounds, especially those in the wavenumber range between 1200 and 600 cm^{-1}. Other bands suggest the presence of other types of bonds or functional groups, such as the one around 2920 cm^{-1} that possibly corresponds to -CH_2. Bands appearing around 2360 cm^{-1} are indicative of axial deformation of double and triple bonds. Several bands were also detected between 1200 and 912 cm^{-1}, which may be ascribed to both the C-O bond of aromatic esters, occurring between 1020 and 1075 cm^{-1}, and the C-OH one characteristic of primary, secondary and tertiary alcohols, usually observed around 1050, 1100 and 1150 cm^{-1}, respectively. Lastly, bands close to 725 cm^{-1} are indicative of aromatic compounds. These results are consistent with those found in the literature, evidencing the occurrence of this class of secondary metabolites in the selected species[29,30].

When compared to the spectrum obtained from the hydroxyethylcellulose analysis, as shown in Figure 11C, we can observe that both share similarities in their composition, with the spectra exhibiting peaks in similar regions, indicating the presence of hydroxyethylcellulose in the dry extract.

When comparing the three spectra, it can be observed that the dry extract shares similarities with the other samples, with bands visible at approximately 2360 cm^{-1}, which is similarly apparent in the crude extract but also exhibits behavior similar to hydroxyethylcellulose. These data suggest both the complex composition of the extracts and their incorporation into the polymer, an idea reinforced by the results of the thermogravimetric analysis.

Conclusion

The ethanolic extract of *M. charantia* Linn. was subjected to HPLC and NMR analyses, which identified phenolic and terpenoid compounds in its composition. Thermal analysis revealed that the drying process was decisive in improving the thermal stability of the dry extract compared to the raw plant material, and FT-IR revealed characteristic bands of the metabolites in both the crude and dry extracts; bands related to hydroxyethylcellulose were also observed, suggesting the success of the polymer incorporation process. Therefore, it is emphasized that the Amazonian variety of *Momordica charantia* has potential for therapeutic use and that spray drying is a viable method to aid in the development of herbal formulations containing the extract.

REFERENCES

1. Stasi LC Di, Hiruma-Lima CA. As plantas medicinais na Amazônia e na Mata Atlântica. 2nd ed. Barbosa NL, Rondinelli M, Seles AS, editors. São Paulo: Editora UNESP; 2003.

2. Ahmad N, Hasan N, Ahmad Z, Zishan M, Zohrameena S. Momordica Charantia: for traditional uses and pharmacological actions. Journal of Drug Delivery and Therapeutics. 2016;6. https://doi.org/10.22270/jddt.v6i2.1202

3. Jiratchariyakul W, Wiwat C, Vongsakul M, Somanabandhu A, Leelamanit W, Fujii I, et al. HIV inhibitor from thai bitter gourd. Planta Med. 2001;67:350–3.

4. Parra AL, Valle RMS, Ferrer JP, Hang PTN, Thi N, Phuong, et al. Antidiabetic, hypolipidemic, antioxidant and anti-inflammatory effects of Momordica charantia L. foliage extract. J Pharm Pharmacogn Res. 2021;9:537–48.

5. Farooqi AA, Khalid S, Tahir F, Uteuliev YS, Yaylim I, Attar R, et al. Bitter gourd (Momordica charantia) as a rich source of bioactive components to combat cancer naturally:

386 Are we on the right track to fully unlock its potential as inhibitor of deregulated signaling
387 pathways. Food and Chemical Toxicology [Internet]. Elsevier; 2018;119:98–105.
388 https://doi.org/10.1016/j.fct.2018.05.024

389 6. Dandawate PR, Subramaniam D, Padhye SB, Anant S. Bitter melon: A panacea for
390 inflammation and cancer. Chin J Nat Med [Internet]. China Pharmaceutical University;
391 2016;14:81–100. https://doi.org/10.1016/S1875-5364(16)60002-X

392 7. Dantas Neto AM, Marinho ML, Leite BMDP de S, Oliveira MG de, Lima ER de.
393 Estudo do efeito acaricida do melão de São Caetano (Momordica charantia) contra Ácaros do
394 tipo Psoroptes ovis e Sarcoptes scabiei. Ciência Animal. 2017;27:42–5.

395 8. Grover JK, Yadav SP. Pharmacological actions and potential uses of Momordica
396 charantia: A review. J Ethnopharmacol. 2004;93:123–32.
397 https://doi.org/10.1016/j.jep.2004.03.035

398 9. Ahamad J, Amin S, R. Mir S. Momordica charantia Linn. (Cucurbitaceae): Review on
399 Phytochemistry and Pharmacology. Research Journal of Phytochemistry. 2017;11:53–65.
400 https://doi.org/10.3923/rjphyto.2017.53.65

401 10. Zannou O, Pashazadeh H, Ghellam M, Ali Redha A, Koca I. Enhanced ultrasonically
402 assisted extraction of bitter melon (Momordica charantia) leaf phenolic compounds using
403 choline chloride-acetic acid–based natural deep eutectic solvent: an optimization approach and
404 in vitro digestion. Biomass Convers Biorefin [Internet]. Springer Science and Business Media
405 Deutschland GmbH; 2022 [cited 2023 Jul 9];1:1–13. https://doi.org/10.1007/S13399-022-
406 03146-0/TABLES/5

407 11. Lopes AP, Galuch MB, Petenuci ME, Oliveira JH, Canesin EA, Schneider VVA, et al.
408 Quantification of phenolic compounds in ripe and unripe bitter melons (Momordica charantia)
409 and evaluation of the distribution of phenolic compounds in different parts of the fruit by
410 UPLC–MS/MS. Chemical Papers. Springer; 2020;74:2613–25.
411 https://doi.org/10.1007/s11696-020-01094-5

412 12. Garcês A, Amaral MH, Sousa Lobo JM, Silva AC. Formulations based on solid lipid
413 nanoparticles (SLN) and nanostructured lipid carriers (NLC) for cutaneous use: A review.
414 European Journal of Pharmaceutical Sciences. Elsevier B.V.; 2018. p. 159–67.
415 https://doi.org/10.1016/j.ejps.2017.11.023

13. Popov P, Honaker LW, Kooijman EE, Mann EK, Jákli AI. A liquid crystal biosensor for specific detection of antigens. Sens Biosensing Res. Elsevier B.V.; 2016;8:31–5. https://doi.org/10.1016/j.sbsr.2016.03.008

14. Nguyen TVL, Nguyen QD, Nguyen PBD, Tran BL, Huynh PT. Effects of drying conditions in low-temperature microwave-assisted drying on bioactive compounds and antioxidant activity of dehydrated bitter melon (Momordica charantia L.). Food Sci Nutr. Wiley-Blackwell; 2020;8:3826–34. https://doi.org/10.1002/fsn3.1676

15. Cano-Higuita D, Vélez H, Telis V. Microencapsulation of turmeric oleoresin Microencapsulation of turMeric oleoresin in binary and ternary blends of guM arabic, Maltodextrin and Modified starch Microencapsulação de oleoresina de cúrcuma em misturas binárias e ternárias de goma arábica, maltodextrina e amido modificado. Ciência e Agrotecnologia. 2015;173–82.

16. Agência Nacional de Vigilância Sanitária. Farmacopeia Brasileira. 6th ed. Brasília; 2019.

17. Pinheiro WBS, Pinheiro Neto JR, Botelho AS, Dos Santos KIP, Da Silva GA, Muribeca AJB, et al. The use of Bagassa guianensis aubl. forestry waste as an alternative for obtaining bioproducts and bioactive compounds. Arabian Journal of Chemistry. Elsevier; 2022;15:103813. https://doi.org/10.1016/J.ARABJC.2022.103813

18. Silva-Júnior JOC, Vieira JLF, Barbosa WLR, Pereira NL. Caracterização físico-química do extrato fluído e seco por nebulização de Symphytum officinale L. Brazilian Journal of Pharmacognosy. 2006;16:671–7.

19. Alves TVG, Costa RS, Gomes ATA, Costa CEF, Perego P, Silva-Júnior JOC, et al. Quality control of amazonian cocoa (Theobroma cacao L.) byproducts and microencapsulated extract by thermal analysis. J Therm Anal Calorim. 2018;

20. Moura AC da S, Santos WVLC dos. Identificação de alguns constituintes quimicos de Indigofera hirsuta LINN. (Fabaceae) por CLAE-IES-EM (TOF) e avaliação da atividade antirradicalar. Quim Nova. 2011;34.

21. Chang C-I, Chen C-R, Liao Y-W, Cheng H-L, Chen Y-C, Chou C-H. Cucurbitane-type triterpenoids from the stems of Momordica charantia. J Nat Prod. 2008;71:1327–30.

22. Liu Y, Ali Z, Khan IA. Cucurbitane-type triterpene glycosides from the fruits of Momordica charantia. Planta Med. 2008;74:1291–4. https://doi.org/10.1177/1934578x1400900327

23. Nhiem NX, Kiem P Van, Minh C Van, Ban NK, Cuong NX, Ha LM, et al. Cucurbitane-type triterpene glycosides from the fruits of Momordica charantia. Magnetic Resonance in Chemistry. 2010;48:392–6. https://doi.org/10.1002/mrc.2582

24. Liao YW, Chen CR, Hsu JL, Cheng HL, Shih WL, Kuo YH, et al. Sterols from the stems of Momordica charantia. Journal of the Chinese Chemical Society. 2011;58:893–8. https://doi.org/10.1002/jccs.201190141

25. Zhang F, Lin L, Xie J. A mini-review of chemical and biological properties of polysaccharides from Momordica charantia. Int J Biol Macromol. 2016;92:246–53. https://doi.org/10.1016/j.ijbiomac.2016.06.101

26. Oliveira MS de, Costa WA da, Bezerra FWF, Araújo ME, Ferreira GC, Carvalho Júnior RN de. Phytochemical profile and biological activities of Momordica charantia L. (Cucurbitaceae): A review. Afr J Biotechnol. Academic Journals; 2018;17:829–46. https://doi.org/10.5897/ajb2017.16374

27. Tran CTH, Wang HMD, Anh LTH, Lin C, Huang CY, Kuo CH. Evaluate the effect of β-cyclodextrin on the sensory and physicochemical properties of bitter gourd extract during thermal processing. Food Chem. Elsevier Ltd; 2024;433. https://doi.org/10.1016/j.foodchem.2023.137394

28. Brandão DO, Guimarães GP, Santos RL, De Júnior FJLR, Da Silva KMA, De Souza FS, et al. Model Analytical Development for Physical, Chemical, and Biological Characterization of Momordica charantia Vegetable Drug. J Anal Methods Chem. Hindawi Limited; 2016;2016. https://doi.org/10.1155/2016/7528297

29. Pham TMH, Ngo D-H, Ngo D-N, Vo TS. Investigation of biological activities of wild bitter melon (Momordica charantia Linn. Var. Abbreviata Ser.). Biomolecules. 2019;9:1–10.

30. Hasan Khan N, Lin ATS, Perveen N. Phytochemical analysis, antibacterial and antioxidant activity determination of Momordica charantia. World J Pharm Pharm Sci. 2019;8:81–96. https://doi.org/10.15406/ppij.2018.06.00223